Combining Thermoelectrics and Low Melting Point Alloys to Create Reconfigurable Stiff-Compliant Manipulators

Emily M. McCabe[1], Daniel S. Esser[1], Tayfun Efe Ertop[1], Alan Kuntz[2], and Robert J. Webster III[1]

***Abstract*— Soft robots have garnered great interest in recent years due to their ability to navigate complex environments and enhance safety during unplanned collisions. However, their softness typically limits the forces they can apply and payloads they can carry, compared to traditional rigid-link robots. In this paper we seek to create a hybrid manipulator that can switch between a state in which it acts as a soft robot, and a state in which it has a series of selectively stiffenable links. The latter state, accomplished by solidifying chambers of low melting point metal alloy within the robot, is in some ways analogous to a traditional rigid-link manipulator. It also has the added benefit that each "link" can be set to a desired straight or curved shape before solidification and re-shaped when desired. Thermoelectric heat pumps enable local heating and cooling of the alloy, and tendons running along the robot enable actuation. Using a simple two-link prototype, we illustrate how alloy melting and solidification can be used to modify the robot's workspace and payload capacity.**

I. INTRODUCTION

Soft robots' ability to continuously bend enables dexterity, obstacle avoidance, and safety during unplanned collisions. Yet the softness of these robots typically limits their payloads and ability to apply forces to their environments. It can thus be advantageous to combine elements of soft and rigid link manipulators (see e.g. [1], among others).

Historically, researchers approached this tradeoff from a rigid-link paradigm, reducing link lengths and increasing the number of links, creating serpentine or hyper-redundant robots [2]–[6]. These researchers even considered the limiting case, from a modeling perspective, of viewing these robots as continuous curves [7]. These robots have been applied or suggested for use in many applications, including farming [8], assembly and maintenance in space [9], inspection of hazardous environments [10], and minimally invasive surgery [11], [12]. However, they have the drawback that they are not truly continuous curves, and they require many actuators, if each link is to be actuated.

Continuum robots (including soft robots) mechanically achieve continuous curves [13], [14]. They accomplish this by incorporating elastic backbones (or being made from soft elastomers) and are underactuated using tendons or other actuators [15], [16]. This makes them adept at compliant grasping and safe when unplanned collisions occur, among other advantages [12]–[17].

Recognizing the complementary advantages of soft and rigid-link robots, researchers have recently explored combining these strategies in two main ways: via alternating rigid-soft components or via stiffening mechanisms within the robot. Conrad et al. used alternating long flexible segments with short rigid-link joints towards the goal of both accuracy and safety in a flexible catheter robot [1]. A variety of approaches to stiffness modulation have been proposed, including granular jamming [18], [19], layer jamming [20], [21], magnetorheological fluids [22], shape memory structures [23], and thermally-activated phase changing materials, including metals, hydrogels, and thermoplastics [24]–[26].

Low melting point alloys (LMPAs) are a particularly interesting emerging approach to stiffening since they provide continuous solid metal elements within the robot when solidified and very soft liquid elements when melted. Candidate metals include Gallium and Bismuth alloys, such as Field's Metal, because their melting temperature is between that of room temperature and boiling water. LMPAs have been incorporated into robots to facilitate grasping and locomotion and have also been suggested for potential future surgical applications [27]–[32], [26], [33]–[36]. The heat required to melt the alloy in these robots has typically been delivered using electrical heating elements, and some have been actively cooled by circulating water through small channels embedded in the robot.

We propose thermoelectric heating and cooling as a way to melt and to solidify the LMPA in such robots, leveraging the Peltier effect. Thermoelectrics are electrically-powered heat pumps. The polarity of the applied current determines the direction that heat is pumped, meaning that a single thermoelectric can be used for both active heating and active cooling. This is the first alternative to circulating water that has been suggested for active cooling in LMPA-based soft robots. Traditionally, Thermoelectric Coolers (TECs) have been used to actively cool electronics, in small refrigerators, and have even been integrated in fabrics to offload excess heat [37]. The closest use of them to the soft robotic application we propose is in custom McKibben actuators where they have been used to vaporize Novec-7000 encased in a silicone balloon [38]. In this paper, we instead utilize both sides of the TECs to move heat from one area of a LMPA-based soft robot to another, leveraging both their heating and cooling effects.

This material is based upon work supported in part by the National Science Foundation (NSF) under grant number 2133027, and in part by the Natural Sciences and Engineering Research Council of Canada (NSERC) under Grant 521537544. Any opinions, findings, and conclusions or recommendations expressed in this material are those of the authors and do not necessarily reflect the views of the NSF or NSERC.

[1]Emily M. McCabe, Daniel S. Esser, Tayfun Efe Ertop, and Robert J. Webster III are with the Department of Mechanical Engineering, Vanderbilt University, Nashville, TN, 37203. (email: Emily.McCabe, Robert.Webster@vanderbilt.edu)

[2]Alan Kuntz is with the Robotics Center and the Kahlert School of Computing at the University of Utah, Salt Lake City, UT 84112, USA.

We use the TECs to create a new kind of manipulator consisting of a series of selectively stiffenable sections (see Fig. 1). In general, these sections can have a variety of lengths. Here, we chose to alternate shorter and longer sections, referring henceforth to the longer ones as "links" and shorter ones as "joints." This choice is made simply for ease of exposition and to underscore the loose analogy to traditional rigid-link robots.

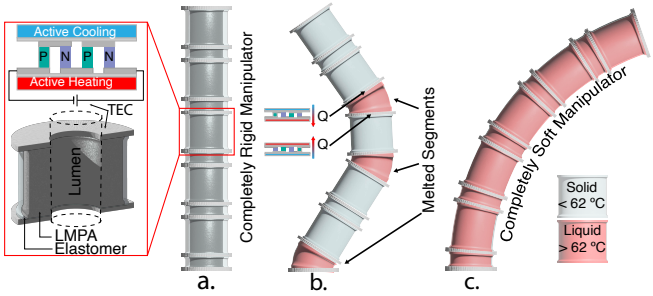

Fig. 1. Robot Concept. (a) The cylindrical manipulator consists of a series of LMPA-filled chambers separated by ring-shaped TECs. (b) The manipulator with some of the joints melted (in red). (c) The manipulator in its fully melted state acts as a soft robot and bends continuously.

When the metal is liquefied, the robot acts as a traditional soft robot. When solidified, it operates in some ways analogously to a rigid link robot. The most closely related work to ours in this sense is that of Alambeigi et al., who used a PTFE-coated spring element to heat a continuous, cylindrical LMPA chamber, running cold water through a central channel for active cooling [26]. They demonstrated the creation of two sections with a "joint" between them by selectively heating different arc length regions of the single cylindrical LMPA chamber using several electrical circuits. Toward improving cycle time, Xing et al. used a somewhat similar two-segment design, but additionally flowed water through a hollow spring for heat exchange, enabling active cooling [35].

Another feature of our design is that we incorporate an open central channel for tool passage, with an eye toward potential future use in minimally invasive surgery. The most closely related prior device in this regard is that of Zhao et al. who designed a stiffening endoscopic overtube [34]. They used a combination of small water and LMPA channels to heat and cool their device, but they did not actively control the device's shape.

In summary, in this paper we contribute (1) the idea of using TECs for active heating and cooling in soft robots, (2) an annular design with a central lumen for tool passage, i.e. combining prior concepts of stiffenable sheath-like robots with LMPA-based stiffening, concepts which have been previously studied individually, but not previously been combined, (3) the idea of a robot that can switch between being a soft robot and being in some ways analogous to a rigid-link robot by solidifying LMPA sections, and (4) a robot with links that are re-shapable by melting them, curving them, and re-solidifying them.

II. Robot Concept and Prototyping

We constructed our prototype from a series of sections separated by TECs. Each TEC was surrounded with a plastic ring containing eylets to support actuation tendons. As noted in the introduction, in general, each section can be any desired length. Here, to reinforce the analogy to traditional robots with rigid links, we choose to alternate between long sections we call "links" (38 mm long) and short sections we call "joints" (15 mm long). The LMPA was encased in an elastomer and its temperature was controlled by the TECs as shown in Fig. 1. Sections melt or solidify as the TECs heat and cool the LMPA adjacent to them. The direction of heat flow can be selected by applying current of the corresponding polarity.

The individual sections of the prototype included three primary components: an annular LMPA core, an elastomeric enclosure, and the TEC devices. The fabrication process involved co-molding the silicone enclosure with the LMPA core (Field's Metal, melting point 62 °C). Geometric parameters of this prototype are shown in Table I.

We 3D printed a two-piece outer mold using PLA (see Fig. 2a) which defined the exterior shape of the silicone. A 3D-printed insert placed concentrically within it was used to define the shape of the internal metal cavity, as well as the inner lumen of the section. We assembled the molds and sealed the interfaces to reduce the presence of air bubbles during the casting and vacuum degassing process. As seen in Fig. 2b, we prepared the silicone *(Smooth-On EcoFlex 00-50)* by mixing and degassing the two-part resin and then injected it into the molds with a syringe. The filled molds were placed in the vacuum chamber to remove any bubbles.

After curing, the silicone was removed from its mold and put into a temperature-controlled chamber to warm prior to the injection, since keeping each component warm helps the LMPA flow into all parts of the silicone before cooling. We melted the LMPA and preheated a glass syringe. The LMPA was suctioned into the syringe and then injected into the warm silicone shell, as shown in Fig. 2c. At this point, the

TABLE I
Prototype Parameters

Component	Parameter	Value
LMPA Core		
	Link Length (l_l)	38 mm
	Joint Length (l_j)	15 mm
	Wall Thickness (t_L)	2 mm
	Outer Radius (R_L)	13 mm
	Inner Radius (r_L)	7 mm
	Contact Surface Area (A_c)	377 mm^2
Silicone Shell		
	Wall Thickness (t_s)	1 mm
	Shore Hardness	00-50
	Modulus (E)	83 kPa
Thermoelectric Cooling Device		
	TEC Length (l_T)	3.8 mm
	Outer Radius (R_T)	13 mm
	Inner Radius (r_T)	7 mm

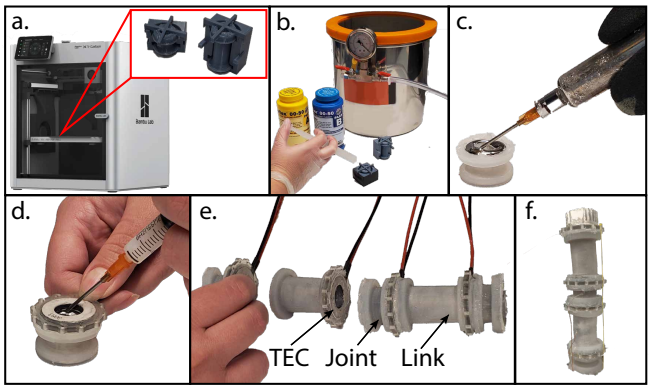

Fig. 2. Prototype fabrication steps: (a) Molds were 3D printed; (b) The silicone shell was cast; (c) The shell was filled with LMPA; (d) The TECs were attached; (e) Link and joint sections were attached in series; (f) The final prototype.

filled silicone was returned to the heating chamber to ensure that all of the metal was heated before being degassed. After the LMPA cooled, the surface of the core was polished to a flat mating surface to ensure no air bubbles were present.

3D-printed tendon guide disks *(Formlabs Clear Resin)* were glued to the circumference of the TECs to support the tendons. These sections were assembled in series as shown in Fig. 2e. At the exposed TEC surfaces at the base and tip, we adhered heat sinks using thermal paste to transfer heat in and out of the prototype. The heat sink at the tip, along with an assembled manipulator, are shown in Fig. 2f.

In this prototype we used the annular TEC RH14-14-06-L1-W4.5 from Laird Thermal Systems. We note that more powerful TECs exist and that TECs can be arranged in other configurations around the LMPA. These particular TECs were selected because they have an open hole through their center, which provides a channel through which a camera or other tools can be delivered.

III. Active Cooling and Phase Transition

TECs are often referred to as heat pumps because they transfer heat from one of their faces to the other. Our goal is to use them to control the temperature of each section in our manipulator, for active heating and cooling. Transition between the liquid and solid phases of the LMPA occurs at 62°C. To measure the temperatures of the individual sections during heating and cooling, we use one Type K thermocouple embedded in the LMPA at the arc length middle of each section. We applied 3.0 A to the TEC, changing the direction as desired to control temperature. Fig. 3, shows the results for heating both links and the joints beyond their melting points. As the heat flows into a section, the LMPA begins with solid heating (initial positive slope), to the phase change (relatively constant temperature), and then to liquid heating (second positive slope). When cooling, these occur in reverse order. During the heating and cooling of any given section, we verified that the adjoining section remains solid.

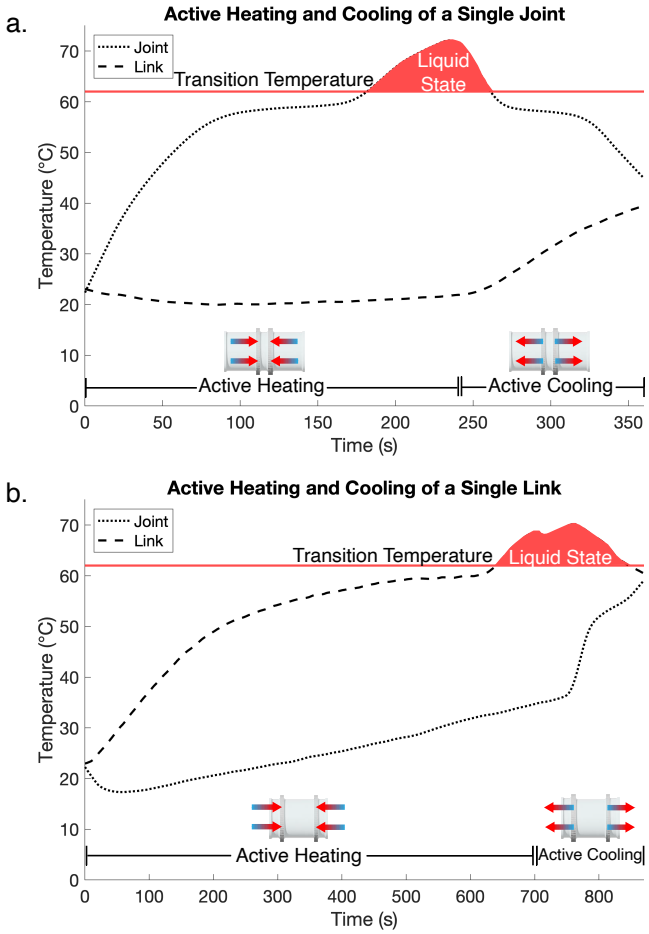

Fig. 3. Heating and cooling of a single joint (top) and link (bottom). The interior temperature is indicated by the dotted line, and the interior temperature of the adjoining link is indicated by the dashed line.

IV. Workspace and Loading Experiments

Here, we characterize the workspace of the manipulator. First, we investigate the achievable workspace of the manipulator under tendon actuation when some or all of the sections are melted, to obtain 11 unique configurations. The individual sections were sequentially heated until the LMPA was in its liquid state. After this, 0.98 N tendon tension was applied. Some example configurations are illustrated in Figure 4. Figure 5 shows all such configurations, plus the fully melted state, superimposed.

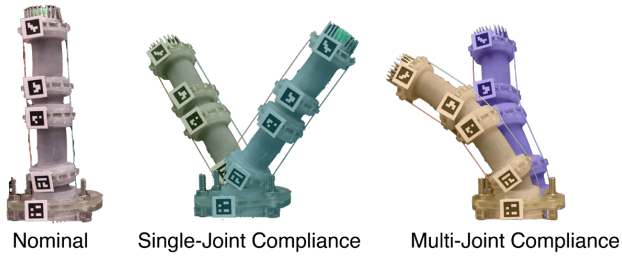

Fig. 4. An illustration of actuating the robot with a single joint liquefied and with multiple joints liquefied.

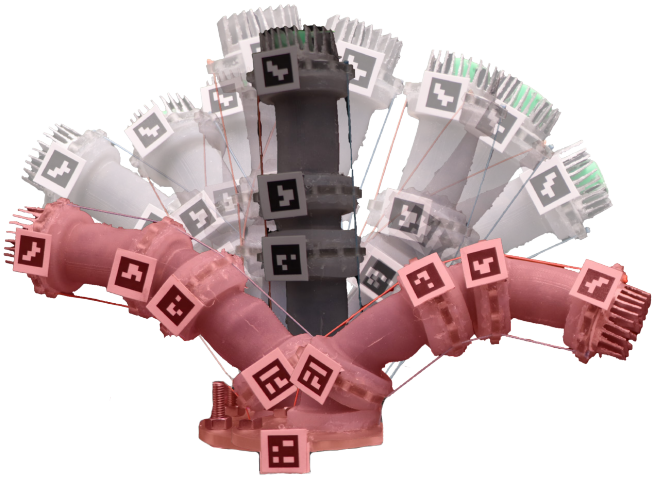

Fig. 5. An illustration of the manipulator's workspace made by superimposing multiple robot configurations with one another. The completely stiff state is shown in black, with states where one or more joints are melted shown in light gray. The completely melted state is shown in red.

To record the change in angle during actuation, we used AprilTag fiducials, to measure the 6 DOF transformations from the base of the manipulator to the tip [39]. When both joints were melted and actuated in the same direction, the maximum tip angle was 65°, and when all sections were melted, it was 115°(see Table II and Fig. 5).

TABLE II

TIP ANGLE UNDER 0.98 N TENDON ACTUATION

	In Plane	Out of Plane
Base Joint	36.5°	-36.7°
Multi-Joint	65.1°	-58.4°
Completely Compliant	114.9°	-80.9°

To explore the ability to carry higher loads with selective stiffening, we characterized the robot's shape under external loads. The tip of the robot was laterally loaded when: (1) the entire robot was soft, (2) the joints were soft and the links were stiff, and (3) the entire robot was stiff (see Fig. 6). The load was applied perpendicularly to the manipulator, at the tip, using a pulley. The tendons were tensioned using 200 g weights tied to each tendon. We applied increasing loads in the liquid/solid configurations until the deformation at the tip exceeded 2 cm. This was found to be at 5 g, 50 g, and 250 g for the completely compliant, compliant joint, and completely rigid states, respectively. Results of the maximum loading cases are shown in Fig. 6.

V. DISCUSSION AND CONCLUSION

In this work we showed that TECs can be used to actively heat and cool link and joint sections in an LMPA-endowed soft robot, while maintaining the phase of the adjoining sections. Note that no attempt has been made in this work to maximize power delivery or to optimize phase transition time. However, since the robot can be moved with tendons once each link and joint is set to the desired stiff/compliant

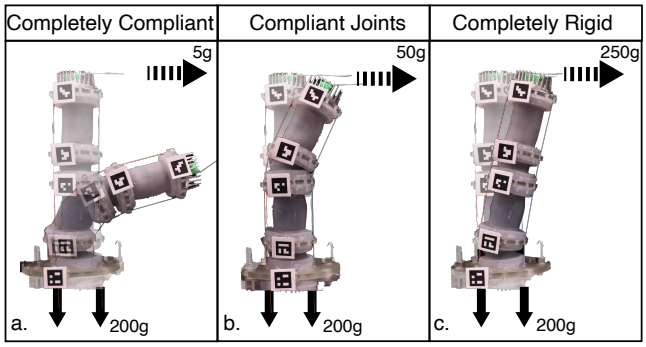

Fig. 6. An illustration of the robot's reaction to external loads. With applied tendon tension of 0.98 N, the manipulator was subjected to point loads at its tip. Final loading conditions for the (a) completely compliant, (b) both joints compliant, and (c) completely rigid states are presented with the payload increasing from left to right.

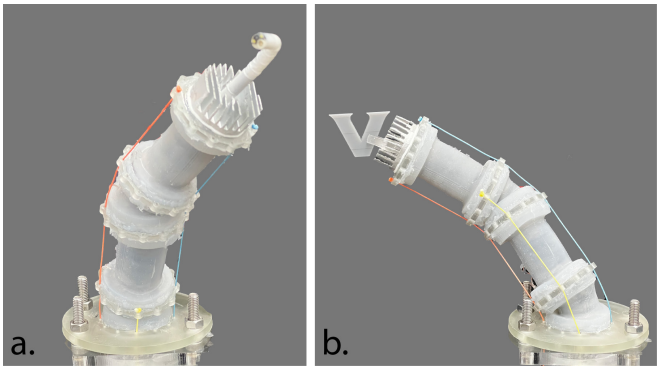

Fig. 7. Illustration of tool delivery. To demonstrate the utility of the inner lumen, we delivered (a) an endoscope for visualization and (b) a grasping end effector.

state, many applications will not be sensitive to the time required for phase transition. The transitions will occur with low frequency – possibly only once at the beginning of a session of robot use. The particular TEC we selected is not the most powerful available, and it was selected mainly for its annular form factor, which facilitates tool passage through the robot. Note that other TECs can be used, along with other arrangements of TECs (e.g. many small TECs could be placed along the outside surface of the robot).

It is also worth noting that we were able to melt the entire robot simultaneously, which may be counter intuitive, since it would not occur from room temperature with ideal heat pumps, since these would only move (not create) heat. However, since our Peltiers are not perfectly efficient, they also generate some waste heat during operation. This effect can be harnessed to raise the temperature of the entire robot when desired.

The annular form factor of our robot facilitates tool deployment. Examples of deploying tools are shown in Fig. 7. This concept was inspired by prior work in stiffening overtubes for surgical robots as discussed in the introduction.

Lastly, we note that the analogy to rigid-link robots is somewhat loose, since our joints are compliant. But the idea of combining the stiffness of rigid link robots with the ability

to become fully soft when desired is the advantage of the design described in this paper. However future work will be needed to demonstrate that our robot can perform tasks that neither a soft nor hyperredundant robot could do alone.

REFERENCES

[1] B. L. Conrad, J. Jung, R. S. Penning, and M. R. Zinn, "Interleaved Continuum-Rigid Manipulation: An Augmented Approach for Robotic Minimally-Invasive Flexible Catheter-Based Procedures," *IEEE International Conference on Robotics and Automation*, pp. 718–724, 2013.

[2] S. Hirose, *Biologically Inspired Robots: Snake-like Locomotors and Manipulators*. Oxford University Press, 1993.

[3] A. Maity, S. K. Mandal, S. Mazumder, and S. Ghosh, "Serpentine Robot: An Overview of Current Status & Prospect," *International Journal on Industrial Robots*, vol. IR32-2, pp. 139–148, 2005.

[4] A. Bayram and M. K. Özgören, "The Conceptual Design of a Spatial Binary Hyper Redundant Manipulator and its Forward Kinematics," *The Institution of Mechanical Engineers, Part C: Journal of Mechanical Engineering Science*, vol. 226, no. 1, pp. 217–227, 2012.

[5] I. Vladu, M. Ivanescu, and I. C. Vladu, "Hyper-Redundant Arm Actuation with Electropneumatic Actuation System: Part I - Construction," *International Conference on System Theory, Control and Computing,*, pp. 573–576, 2013.

[6] K. Ning and F. Wörgötter, "A novel concept for building a hyper-redundant chain robot," *IEEE Transactions on Robotics*, vol. 25, no. 6, pp. 1237–1248, 2009.

[7] G. S. Chirikjian and J. W. Burdick, "The Kinematics of Hyper-Redundant Robot Locomotion," *IEEE Transactions on Robotics And Automation*, vol. 11, no. 6, 1995.

[8] C. Lapusan, C. Rad, and O. Hancu, "Kinematic Analysis of a Hyper-Redundant Robot with Application in Vertical Farming," *IOP Conference Series: Materials Science and Engineering*, vol. 1190, 2021.

[9] G. S. Chirikjian and J. Burdick, "Applications of Hyper-Redundant Manipulators for Space Robotics and Automation," *International Symposium on Artificial Intelligence, Robotics and Automation in Space*, pp. 291–294, 1990.

[10] G. S. Chirikjian, "Hyper-redundant Manipulator Dynamics: a Continuum Approximation," *Advanced Robotics*, vol. 9, no. 3, pp. 217–243, 1994.

[11] N. Simaan, R. Taylor, and P. Flint, "A Dexterous System for Laryngeal Surgery," *IEEE International Conference on Robotics and Automation*, vol. 1, no. 1, pp. 351–357, 2004.

[12] J. Burgner-Kahrs, D. C. Rucker, and H. Choset, "Continuum Robots for Medical Applications: A Survey," *IEEE Transactions on Robotics*, vol. 31, no. 6, pp. 1261–1280, 2015.

[13] R. J. Webster III and B. A. Jones, "Design and Kinematic Modeling of Constant Curvature Continuum Robots: A Review," *The International Journal of Robotics Research*, vol. 29, no. 13, pp. 1661–1683, 2010.

[14] D. Trivedi, A. Lotfi, and C. Rahn, "Geometrically Exact Models for Soft Robotic Manipulators," *IEEE Transactions on Robotics*, vol. 24, no. 4, pp. 773–780, 2008.

[15] M. Russo, S. Mohammad, H. Sadati, X. Dong, A. Mohammad, I. D. Walker, C. Bergeles, K. Xu, and D. A. Axinte, "Continuum Robots: An Overview," *Advanced Intelligent Systems*, vol. 5, no. 5, p. 2200367, 2023.

[16] I. A. Seleem, H. El-Hussieny, and H. Ishii, "Recent Developments of Actuation Mechanisms for Continuum Robots: A Review," *International Journal of Control, Automation, and Systems*, vol. 21, no. 5, pp. 1592–1609, 2023.

[17] I. D. Walker, J. Archibald, and J. B. Koeneman, "Continuous Backbone "Continuum" Robot Manipulators," *International Scholarly Research Notices*, pp. 1–19, 2013.

[18] M. Cianchetti, T. Ranzani, G. Gerboni, T. Nanayakkara, K. Althoefer, P. Dasgupta, and A. Menciassi, "Soft Robotics Technologies to Address Shortcomings in Today's Minimally Invasive Surgery: The STIFF-FLOP Approach," *Soft Robotics*, vol. 1, no. 2, pp. 122–131, 2014.

[19] N. G. Cheng, M. B. Lobovsky, S. J. Keating, A. M. Setapen, K. I. Gero, A. E. Hosoi, and K. D. Iagnemma, "Design and Analysis of a Robust, Low-Cost, Highly Articulated Manipulator Enabled by Jamming of Granular Media," *IEEE International Conference on Robotics and Automation*, pp. 4328–4333, 2012.

[20] Y. J. Kim, S. Cheng, S. Kim, and K. Iagnemma, "A Novel Layer Jamming Mechanism with Tunable Stiffness Capability for Minimally Invasive Surgery," *IEEE Transactions on Robotics*, vol. 29, no. 4, pp. 1031–1042, 2013.

[21] B. H. Do, V. Banashek, and A. M. Okamura, "Dynamically Reconfigurable Discrete Distributed Stiffness for Inflated Beam Robots," *IEEE International Conference on Robotics and Automation*, pp. 9050–9056, 2020.

[22] X. Yin, J. Yan, S. Wen, and J. Zhang, "Magnetorheological Fluid-Filled Origami Joints With Variable Stiffness Characteristics," *IEEE/ASME Transactions on Mechatronics*, vol. 28, no. 3, pp. 1546–1557, 6 2023.

[23] Y. Cao, F. Ju, L. Zhang, D. Bai, F. Qi, and B. Chen, "A Novel Variable-Stiffness Flexible Manipulator Actuated by Shape Memory Alloy for Minimally Invasive Surgery," *The Institution of Mechanical Engineers, Part H: Journal of Engineering in Medicine*, vol. 232, no. 11, pp. 1098–1110, 2018.

[24] D. G. Mosquera, S. H. Sadati, K. Althoefer, and T. Nanayakkara, "Smart Hydrogel for Stiffness Controllable Continuum Manipulators: A Conceptual Design," *Soft and Stiffness-Controllable Robotics Solutions for Minimally Invasive Surgery*, pp. 79–96, 2022.

[25] H. M. Le, L. Cao, T. N. Do, and S. J. Phee, "Design and Modelling of a Variable Stiffness Manipulator for Surgical Robots," *Mechatronics*, vol. 53, pp. 109–123, 2018.

[26] F. Alambeigi, R. Seifabadi, and M. Armand, "A Continuum Manipulator with Phase Changing Alloy," in *2016 IEEE International Conference on Robotics and Automation (ICRA)*, 2016, pp. 758–764.

[27] Y. Hao, T. Wang, X. Fang, K. Yang, L. Mao, J. Guan, and L. Wen, "A Variable Stiffness Soft Robotic Gripper with Low-Melting-Point Alloy," *Chinese Control Conference*, pp. 6781–6786, 2017.

[28] G. Chen, B. Ma, J. Zhang, Y. Chen, and H. Liu, "Reprogrammable Magnetic Soft Robots Based on Low Melting Alloys," *Advanced Intelligent Systems*, vol. 5, no. 10, p. 2300173, 2023.

[29] W. Wang and S. H. Ahn, "Shape Memory Alloy-Based Soft Gripper with Variable Stiffness for Compliant and Effective Grasping," *Soft Robotics*, vol. 4, no. 4, pp. 379–389, 2017.

[30] M. D. Christie, S. Sun, D. H. Ning, H. Du, S. W. Zhang, and W. H. Li, "A Highly Stiffness-Adjustable Robot Leg for Enhancing Locomotive Performance," *Mechanical Systems and Signal Processing*, vol. 126, pp. 458–468, 2019.

[31] R. L. Baines, J. W. Booth, F. E. Fish, and R. Kramer-Bottiglio, "Toward a Bio-Inspired Variable-Stiffness Morphing Limb for Amphibious Robot Locomotion," *IEEE International Conference on Soft Robotics*, pp. 704–710, 2019.

[32] R. Zhao, H. Dai, and H. Yao, "Liquid-Metal Magnetic Soft Robot with Reprogrammable Magnetization and Stiffness," *IEEE Robotics and Automation Letters*, vol. 7, no. 2, pp. 4535–4541, 2022.

[33] T. Thien Hoang, P. Thien Phan, M. Thanh Thai, N. H. Lovell, T. Nho Do, T. T. Hoang, P. T. Phan, M. T. Thai, N. H. Lovell, and T. N. Do, "Bio-Inspired Conformable and Helical Soft Fabric Gripper with Variable Stiffness and Touch Sensing," *Advanced Materials Technologies*, vol. 5, no. 12, p. 2000724, 2020.

[34] R. Zhao, Y. Yao, and Y. Luo, "Development of a Variable Stiffness Over Tube Based on Low-Melting-Point-Alloy for Endoscopic Surgery," *ASME Journal of Medical Devices*, vol. 10, no. 2, 2016.

[35] Z. Xing, F. Wang, Y. Ji, D. McCoul, X. Wang, and J. Zhao, "A Structure for Fast Stiffness-Variation and Omnidirectional-Steering Continuum Manipulator," *IEEE Robotics and Automation Letters*, vol. 6, no. 2, pp. 755–762, 2021.

[36] J. Zhang, B. Wang, H. Chen, J. Bai, Z. Wu, J. Liu, H. Peng, and J. Wu, "Bioinspired Continuum Robots with Programmable Stiffness by Harnessing Phase Change Materials," *Advanced Materials Technologies*, vol. 8, no. 6, 2023.

[37] W.-Y. Chen, X.-L. Shi, J. Zou, Z.-G. Chen, W.-Y. Chen, X.-L. Shi, J. Zou, and Z.-G. Chen, "Thermoelectric Coolers: Progress, Challenges, and Opportunities," *Small Methods*, vol. 6, no. 2, p. 2101235, 2022.

[38] T. Exley, D. Johnson, and A. Jafari, "Utilizing the Peltier Effect for Actuation of Thermo-Active Soft Robots," *Smart Materials and Structures*, vol. 32, no. 8, p. 085029, 2023.

[39] E. Olson, "AprilTag: A Robust and Flexible Visual Fiducial System," *IEEE International Conference on Robotics and Automation*, pp. 3400–3407, 2011.